Journal of Magnetic Resonance **142,** 288–293 (2000)
doi:10.1006/jmre.1999.1951, available online at http://www.idealibrary.com on IDEAL®

3D $HCCH_3$-TOCSY for Resonance Assignment of Methyl-Containing Side Chains in ^{13}C-Labeled Proteins

Dušan Uhrín,*[,1] Stanislava Uhrínová,* Claire Leadbeater,* Jacqueline Nairn,† Nicholas C. Price,† and Paul N. Barlow*

*The Edinburgh Centre for Protein Technology, Department of Chemistry, The University of Edinburgh, West Mains Road, Edinburgh, EH9 3JJ, United Kingdom; and †Department of Biological and Molecular Sciences, University of Stirling, Stirling FK9 4LA, United Kingdom

Received May 25, 1999

Two 3D experiments, (H)CCH_3-TOCSY and H(C)CH_3-TOCSY, are proposed for resonance assignment of methyl-containing amino acid side chains. After the initial proton–carbon INEPT step, during which either carbon or proton chemical shift labeling is achieved (t_1), the magnetization is spread along the amino acid side chains by a carbon spin lock. The chemical shifts of methyl carbons are labeled (t_2) during the following constant time interval. Finally the magnetization is transferred, in a reversed INEPT step, to methyl protons for detection (t_3). The proposed experiments are characterized by high digital resolution in the methyl carbon dimension (t_{2max} = 28.6 ms), optimum sensitivity due to the use of proton decoupling during the long constant time interval, and an optional removal of CH_2, or CH_2 and CH, resonances from the F_2F_3 planes. The building blocks used in these experiments can be implemented in a range of heteronuclear experiments focusing on methyl resonances in proteins. The techniques are illustrated using a ^{15}N, ^{13}C-labeled E93D mutant of *Schizosacharomyces pombe* **phosphoglycerate mutase (23.7 kDa).**

Key Words: **3D NMR; HCCH-TOCSY; protein side chains; methyl-containing amino acids.**

Methyl-containing amino acids occur frequently in protein interiors and are abundant at molecular interfaces (*1*). Mapping of the inter residue NOEs arising from methyl-containing side chains plays an important role in the determination of the structures of proteins by NMR. In recognition of this fact, several recent papers have suggested customizing 3D ^{13}C-edited NOE experiments so as to focus on the methyl groups (*2–4*). A prerequisite for the effective use of such NOE data is a complete or a near complete resonance assignment of methyl-containing residues. The usual route for the side chain resonance assignment of ^{15}N, ^{13}C proteins is via ^{13}C–^{13}C TOCSY-based experiments (*5–10*). Among these, two NH-detected experiments, (H)C(CO)NH-TOCSY and H(C)(CO)NH-TOCSY (*9, 10*), are the most widely used. Here the magnetization transfer is directed from H–C moieties to NH protons. Such methods are general and work for all amino acids except for instances where an amino acid is preceded by a proline.

We present here two 3D experiments, (H)CCH_3-TOCSY and H(C)CH_3-TOCSY, designed specifically for side chain resonance assignment of methyl-containing residues and schematically diagrammed in Fig. 1. The initial parts of the pulse sequences (Figs. 2A and 2B) are formally identical to those of the (H)C(CO)NH-TOCSY (*11*) and H(C)(CO)NH-TOCSY (*10*) experiments. The methyl-selected experiments differ only after the carbon spin-lock period when the carbon magnetization is not directed to NH protons but instead ends up on CH_3 protons (t_3). The chemical shift-labeling of methyl carbons (t_2) is achieved during the constant time period, T, preceded by chemical shift-labeling of side chain proton or carbon resonances (t_1). When we first applied these experiments (*12*) we employed a short T interval (9.6 ms); the methyl carbon chemical shift modulation was achieved by incrementing a pair of 180° pulses within this interval and no attempt was made to select only methyl resonances. We report here several modifications which greatly improve the performance of the original technique: (i) longer constant time interval for chemical shift-labeling of methyl carbons (Fig. 2C) resulting in a superior resolution of resonances in this dimension; (ii) proton spin-flips during most of this interval are eliminated (Fig. 2D), reducing the detrimental effects of relaxation; (iii) an optional removal of CH_2 (Fig. 2E), or CH and CH_2 (Fig. 2F), resonances from F_2F_3 planes is presented. In the following, these modifications are described and illustrated using a ^{15}N, ^{13}C-labeled E93D mutant of *Schizosacharomyces pombe* phosphoglycerate mutase (*13*) (E93D-PGAM, 23.7 kDa).

In order to take full advantage of the inherently good separation of methyl cross peaks in proton–carbon correlated spectra of proteins, it is desirable to lengthen the ^{13}C chemical shift-labeling of methyl groups while not compromising the sensitivity of the experiments. The transfer function for CH_3 groups during the constant time period, T, of the experiment shown in Fig. 2C is given by I, where

$$I = 3\,\sin(\pi {}^1J_{CH}\Delta_1)\cos^2(\pi {}^1J_{CH}\Delta_1) \times \cos(\pi {}^1J_{CC}T)\exp(-T/T_2).$$

The relaxation time, T_2, includes contributions from spin-flips

[1] To whom correspondence should be addressed.

1090-7807/00 $35.00

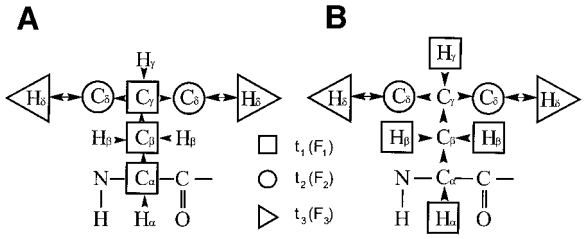

FIG. 1. Schematic representation of the flow of magnetization in (A) (H)CCH$_3$-TOCSY and (B) H(C)CH$_3$-TOCSY.

of methyl protons and from transverse relaxation of in-phase methyl carbon magnetization. When delay Δ_1 is optimized for CH_3 groups ($\Delta_1 = 1.6$ ms, $^1J_{CH} = 123$ Hz, $^1J_{CC} = 35$ Hz) and relaxation is neglected, I takes on values of 0.57, -0.57, and -1.15 for T of 9.6, 19.0, and 28.6 ms, respectively. The first setting was used in an original experiment (*12*) during the resonance assignment of the protein β-lactoglobuline (18.4 kDa). The last is the global maximum corresponding to the time interval of $1/J_{CC}$ (*14*, *15*). As a consequence of the slow relaxation of methyl carbons (*16*), it is often possible to use the global maximum and to lengthen the T interval without losing too much signal (*4*).

Replacement of a pair of 180° proton and carbon pulses by heteronuclear decoupling (Fig. 2D) eliminates the proton spin-flips (*17*) and results in a significant gain in sensitivity (compare Figs. 3a and 3b), especially when a longer T period is employed. This modification is straightforward, since the carbon magnetization is in-phase after the carbon spin-lock period. The optimum value of T is obtained by balancing sensitivity and resolution in the methyl carbon dimension. The sensitivity can be checked experimentally by recording the first

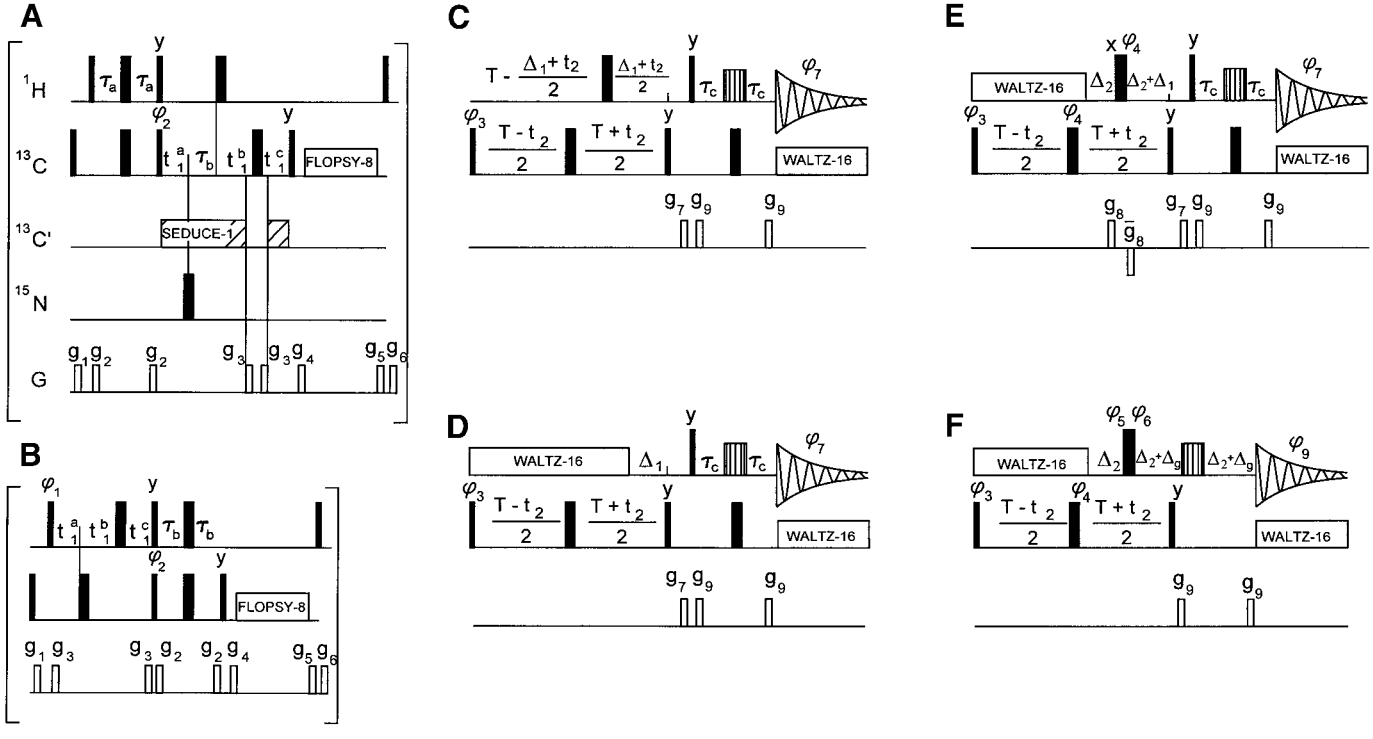

FIG. 2. Pulse sequences of (H)CCH$_3$-TOCSY [A + C, or D, E, F] and H(C)CH$_3$-TOCSY [B + C, or D, E, F] experiments. Narrow and wide bars represent 90° and 180° x axis pulses unless indicated otherwise. The ^{1}H, ^{15}N, and ^{13}C, carriers are, at the beginning of the pulse sequences, centered at 2.5, 120, and 43 ppm, respectively. The ^{1}H and ^{13}C frequencies were changed to 1.1 and 20 ppm, respectively, after the FLOPSY-8 sequence (*21*). All gradient pulses are applied along the z direction with the exception of WATERGATE (*22*) gradient pulses which are applied along the z and y axes. The carbonyl decoupling is achieved using a 134-ppm cosine-modulated (*23*) WALTZ-16 (*24*) field with 320-μs 90° pulses having SEDUCE (*25*) shapes. The delays employed are as follows: $\tau_a = 1.8$ ms, $\tau_b = 0.9$ ms, $\tau_c = 2.0$ ms, $\Delta_1 = 1.6$ ms, $\Delta_2 = 4.0$ ms. Recommended values for T are 28.6, 19.0, or 9.6 ms, preference in the order given, and Δg is the duration of the g_9 gradient. In the experiment (A) the additional delays are $t_1^a = t_1/2$, $t_1^b = t_1/2 + \delta$, and $t_1^c = \tau_b + \delta$; $\delta = \Delta g_3 + 2\text{pw} - n\tau_b/(N - 1)$, where Δg_3 is the duration of the gradient g_3, pw is the ^{1}H 90° pulse, N is the number of complex points in the ^{13}C dimension, $n = 0, 1, 2 \ldots (N - 1)$. In experiment (B) the additional delays are $t_1^a = t_1/2 + \tau_a$, $t_1^b = t_1/2 + \delta$, and $t_1^c = \tau_a + \delta$; $\delta = 2\text{pwc} - n(\tau_a - \Delta g_3)/(N - 1)$, where pwc is the ^{13}C 90° pulse. Quadrature detection in F_1 and F_2 is achieved via States–TPPI (*26*, *27*) of φ_2 and φ_3 or φ_1 and φ_3. The phase cycling is $\varphi_1 = x$; $\varphi_2 = x, -x$; $\varphi_3 = x$; $\varphi_4 = 2x, 2(-x)$; $\varphi_5 = 30°$; $\varphi_6 = 2(0°), 2(60°), 2(120°), 2(180°), 2(240°), 2(300°)$; $\varphi_7 = x, -x$; $\varphi_8 = x, 2(-x), x$; $\varphi_9 = 0°, 180°, 120°, 300°, 240°, 60°$. The duration and the strength of the gradients are: $g_1 = 1$ ms, 10 G/cm, $g_2 = 0.5$ ms, 7 G/cm, $g_3 = 0.2$ ms, 15 G/cm, $g_4 = 0.29$ ms, 22 G/cm, $g_5 = 0.5$ ms, 22 G/cm, $g_6 = 0.5$ ms, 26.4 G/cm, $g_7 = 0.5$ ms, 18 G/cm, $g_8 = 0.8$ ms, 10 G/cm, $\overline{g_8} = 0.8$ ms, -10 G/cm, $g_9 = 0.5$ ms, 40 G/cm. The use of the 90° proton pulse after the gradient g_5 followed by the gradient g_6 improves water suppression.

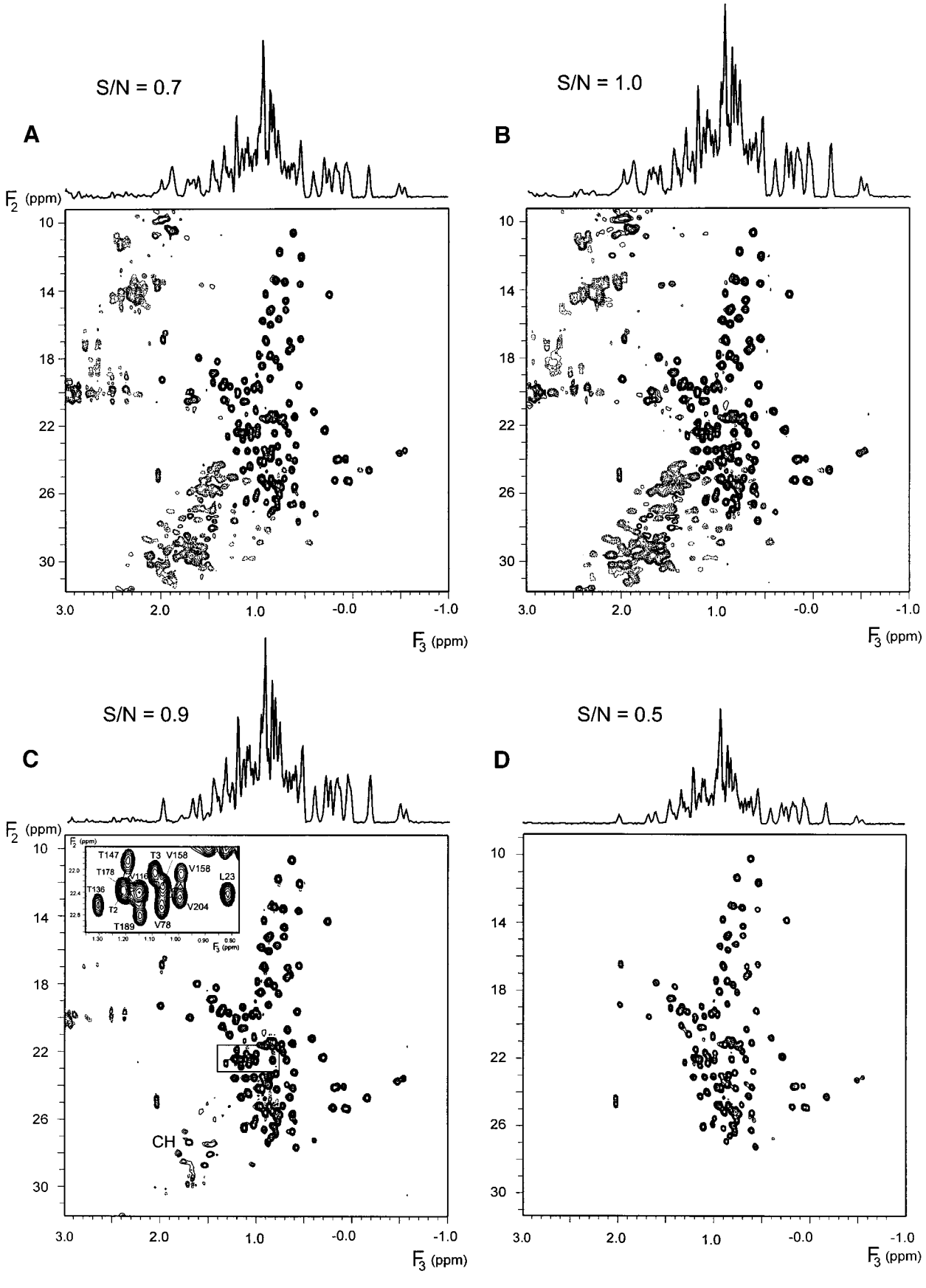
A
S/N = 0.7
B
S/N = 1.0
C
S/N = 0.9
D
S/N = 0.5
F2 (ppm)
F3 (ppm)
10
14
18
22
26
30
3.0
2.0
1.0
-0.0
-1.0
T147
T3
V158
T178
V116
T136
T2
T189
V78
V204
L23
CH

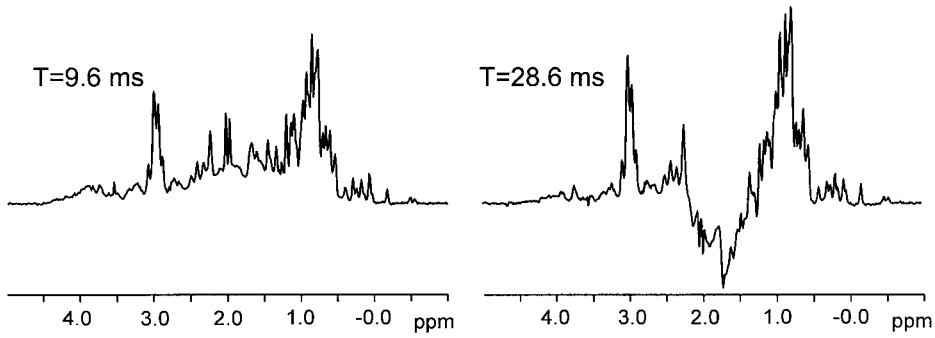

FIG. 4. 1D spectra of E93D-PGAM acquired using the pulse sequence A + D of Fig. 2 without the SEDUCE decoupling and FLOPSY spin-lock. The constant time interval, T, was set to 9.6 and 28.6 ms, respectively. Number of scans was 64, $t_1 = t_2 = 0$.

1D trace of a 3D spectrum using several values of T. Such a comparison for E93D-PGAM at 37°C shows (Fig. 4) that the signals for most of the methyl groups are more intense when the longer T period is used. The resolution can be assessed by acquiring the first F_2F_3 plane of a 3D experiment (Fig. 3).

The third class of modifications concerns removal of the signals due to CH_2, or CH and CH_2, resonances from the methyl proton–carbon planes. In instances where CH_3 resonances overlap with CH_2 or CH resonances, the original experiments may fail to yield the resonance assignment. The CH_2 resonances are more likely to overlap with some of the methyl resonances than are the CH resonances, the latter belonging mostly to C_γ of Leu. Considering this, two modifications were designed. The first modification (Fig. 2E), which eliminates only the CH_2 resonances, exploits the different behavior of coherences due to the odd or even number of carbon-bound protons (*18*). Zero or 180° proton pulses are applied on alternate scans when $S_xI_{1/z}$, $S_xI_{1/z}$, $I_{2/z}$ and $S_xI_{1z}I_{2z}I_{3z}$ states of CH, CH_2, and CH_3 groups, respectively, were created. The resulting changes in the sign of the S_xI_{1z} and $S_xI_{1z}I_{2z}I_{3z}$ coherences are followed by the receiver, thus eliminating the signal from the CH_2 groups. Only a minor decrease in signal intensities (<10%) compared with the nonedited experiment occurred as a result of the editing (compare Figs. 3B and 3C). Artifacts arising from imperfect 0°/180° editing proton pulses were eliminated by surrounding them by a pair of equally strong gradients applied with different polarity. It was thereby possible to keep the minimum number of scans per increment at four in this pulse sequence.

Elimination of both CH and CH_2 resonances was achieved by a heteronuclear quadruple-quantum (HQQ) filter using phase cycling (*19*) rather than pulsed field gradients (*2*) (Fig. 2F). This prevents sensitivity losses due to the coherence selection by gradients; however, it results in a longer phase cycling. The minimum number of scans per increment in this 3D experiment is 12. This is still acceptable, given the small spectral width in the methyl carbon dimension. While removal of the CH_2 signals had minimal effect on the sensitivity of the experiments, the use of the HQQ filter is accompanied by a loss of approximately one-half of the signal compared to the nonedited experiments. This is mostly a consequence of preparing the HQQ coherence from in-phase carbon magnetization (*19*) ($S_y \rightarrow -8S_xI_{1y}I_{2y}I_{3y}$). The theoretical S/N ratio achievable in this arrangement is 65% of that obtained in the reverse INEPT. We note that the S/N ratio of a phase-cycled HQQC experiment (*20*) which utilizes the $2S_yI_{1x} \rightarrow -8S_yI_{1x}I_{2y}I_{3y}$ pathway is 75% of the regular HSQC experiment; however, only the former scheme can be efficiently implemented into our pulse sequences. Despite the use of phase cycling, and therefore reliance on signal cancellation, rather than gradient selection, very clean spectra were obtained (Fig. 3D).

Out of 211 residues in E93D-PGAM, 78 contain a total of 127 methyl groups. Due to the high resolution in the carbon methyl dimension, 110 methyl cross peaks were resolved in the 3D spectra. CH_3 strips from such 3D spectra can be easily extracted even for closely spaced resonances belonging to residues of the same kind. Methyl cross peaks of six threonine and five valine residues resonating in a small frequency space ($F_2 \times F_3 = 1.0 \times 0.3$ ppm) are shown in the inset of Fig. 3c. Corresponding F_1F_3 strips from two HCCH$_3$-TOCSY spectra are shown in Fig. 5. Even overlapping cross peaks of residues T2 and T178 were sufficiently unique that it was possible to assign signals of their C_α and C_β carbons (Fig. 5A). Such digital resolution is obtained in a very short time. When using 0.4–1.0

FIG. 3. Proton–carbon CH_3 planes of the (H)CCH$_3$-TOCSY acquired on E93-PGAM (1 mM, 300 μL, 5-mm Shigemi tube, 37°C) using the pulse sequences of Fig. 2. The (A–D) spectra were recorded using the A + C, D, E, F pulse sequences, respectively. The CH_2 signals are shown using dashed lines. The following acquisition parameters were used: T = 28.6 ms, spectral width in F_2 and F_3 were 3400 and 5000 Hz, acquisition time t_3 = 63 ms, t_{2max} = 28.24 ms, 8 transients were acquired per each of 96 increments except for (D), where 12 scans were accumulated; relaxation delay was 1.2 s. The total acquisition time was 33 min (50 in (D)). Relative numbers for the signal-to-noise ratio obtained from the analysis of 1D traces of 20 cross peaks, corrected for the larger number of scans in (D), are given for each spectrum. The inset of (C) shows cross peaks for which the F_1F_3 strips were extracted (Fig. 5) from two 3D HCCH$_3$-TOCSY spectra.

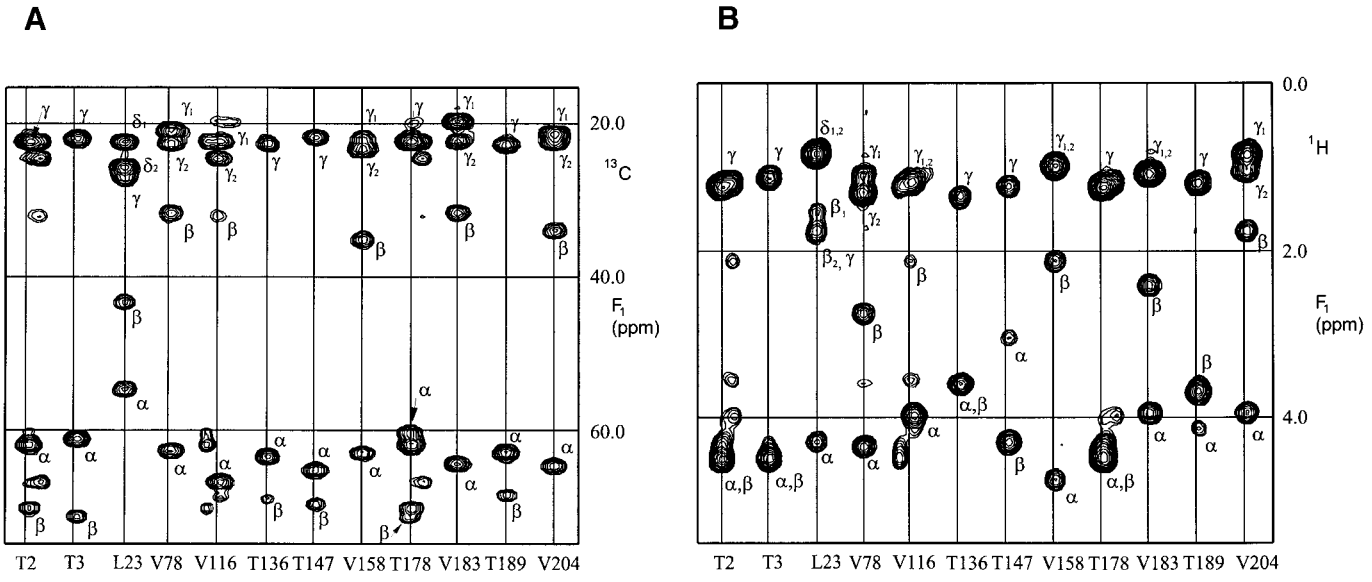

FIG. 5. ^{13}C methyl strips from (A) (H)CCH$_3$-TOCSY and (B) H(C)CH$_3$-TOCSY spectra acquired on a E93D-PGAM (1 mM, 300 μL, 5-mm Shigemi tube, 37°C) using the pulse sequences of Figs. 2A + 2E and 2B + 2E, respectively. Strips through cross peaks shown in the inset of the Fig. 3c are presented. The following parameters were used to acquire the spectra: spectral width in F_2 and F_3 were 3400 and 5000 Hz, acquisition time t_3 = 63 ms, t_{2max} = 28.24 ms, 4 transients were acquired per increment, relaxation time was 1.2 s. The carbon spin-lock time was 19 ms. Spectral widths in $F_1(t_{1max})$ were 4200 Hz (10.5 ms) and 10,560 Hz (6.5 ms) for proton and carbon chemical shift recorded experiments, respectively. The total acquisition times were 25 and 36 h, respectively.

mM protein concentrations, 24 and 36 h are usually sufficient to acquire high-quality 3D H(C)CH$_3$-TOCSY and (H)CCH$_3$-TOCSY spectra, respectively.

The experiments proposed here offer several advantages over methods based on NH detection. The intensities of cross peaks in the methyl-detected experiments are higher than in NH-detected methods, an observation which can be attributed to the shorter and more efficient polarization transfer pathway in the former experiments. Because the magnetization from side chains in HC(CO)NH-TOCSY-type experiments is detected on NH protons of the subsequent residue, side chain resonances of residues preceding prolines are not accessible in such experiments. Overlaps in ^{1}H–^{15}N HSQC spectra cause ambiguities when only NH-detected experiments are used. An additional advantage of the methyl-detected experiments accrues from the fact that there is, inherently, proton–carbon correlation information for CH$_3$ groups which is not present in the NH-detected spectra. This is important for assigning methyl proton and carbon resonances for residues with two CH$_3$ groups such as Val, Leu, and Ile. In the methyl-detected experiments these resonances are present in two different strips, except where both methyls have the same carbon and proton shifts. This also allows verification of the assignments and removal of possible ambiguities arising from overlap with resonances from other residues. A potential drawback of the CH$_3$-detected experiments is that the identity of the amino acids can be established only by comparison with α and β proton and carbon chemical shifts obtained during the backbone assignment. Inherently, only resonance assignment of methyl-containing side chains is obtained.

In conclusion, two sensitive experiments have been proposed for side chain resonance assignment of methyl-containing residues. High digital resolution in the methyl carbon dimension, optimized sensitivity due to the elimination of proton spin-flips during the long constant time interval, and a possibility of removal of the CH$_2$, or CH$_2$ and CH, signals constitute significant improvements of our original experiments (*12*). The proposed modifications can be implemented into a range of heteronuclear experiments which focus on methyl resonances in proteins.

ACKNOWLEDGMENTS

This project was supported by the Wellcome Trust and the Edinburgh Centre for Protein Technology. We thank Dr. Tibor Liptaj for useful discussions during the course of this project and Doris Duncan for help with the preparation of the protein.

REFERENCES

1. J. Janin, S. Miller, and C. Chothia, Surface, subunit interfaces and interior of oligomeric proteins, *J. Mol. Biol.* **204,** 155–164 (1988).
2. T. Diercks, M. Schwaiger, and H. Kessler, HSQC-based methyl group selection via gradients in multidimensional NMR spectroscopy of proteins, *J. Magn. Reson.* **130,** 335–340 (1998).
3. C. Zwahlen, S. J. F. Vincent, K. H. Gardner, and L. E. Kay, Significantly improved resolution for NOE correlations from valine and isoleucine (C$^{\gamma 2}$) methyl groups in ^{15}N, ^{13}C and ^{15}N, ^{13}C ^{2}H-labelled proteins, *J. Am. Chem. Soc.* **120,** 4825–4831 (1998).
4. C. Zwahlen, K. H. Gardner, S. P. Sarma, D. A. Horita, R. A. Byrd, and L. E. Kay, An NMR experiment for measuring methyl–methyl

NOEs in ^{13}C-labelled proteins with high resolution, *J. Am. Chem. Soc.* **120,** 7617–7625 (1998).

5. S. W. Fesik, H. L. Eaton, E. T. Olejniczak, and E. R. P. Zuiderweg, 2D and 3D NMR spectroscopy employing ^{13}C–^{13}C magnetization transfer by isotropic mixing. Spin system identification in large proteins, *J. Am. Chem. Soc.* **112,** 886–888 (1990).
6. A. Bax, G. M. Clore, and A. M. Gronenborn, ^{1}H–^{1}H correlation via isotropic mixing of ^{13}C magnetisation, a new 3-dimensional approach for assigning ^{1}H and ^{13}C spectra of ^{13}C-enriched proteins, *J. Magn. Reson.* **88,** 425–431 (1990).
7. G. T. Montelione, B. A. Lyons, S. D. Emerson, and M. Tashiro, An efficient triple resonance experiment using carbon-13 isotropic mixing for determining sequence-specific resonance assignment of isotopically-enriched proteins, *J. Am. Chem. Soc.* **114,** 10974–10975 (1992).
8. T. M. Logan, E. T. Olejniczak, R. X. Xu, and S. W. Fesik, Side-chain and backbone assignments in isotopically labelled proteins from two heteronuclear tripple-resonance experiments, *FEBS Lett.* **314,** 413–418 (1992).
9. T. M. Logan, E. T. Olejniczak, R. X. Xu, and S. W. Fesik, A general method for assigning NMR spectra of denatured proteins using 3D HC(CO)NH-TOCSY triple resonance experiments, *J. Biomol. NMR* **3,** 225–231 (1993).
10. S. Grzesiek, J. Anglister, and A. Bax, Correlation of backbone amide and aliphatic side-chain resonances in ^{13}C/^{15}N-enriched proteins by isotropic mixing of ^{13}C-magnetization, *J. Magn. Reson. B* **101,** 114–119 (1993).
11. K. H. Gardner, R. Konrat, M. K. Rosen, and L. E. Kay, An (H)C(CO)NH-TOCSY pulse scheme for sequential assignment of protonated methyl groups in otherwise deuterated ^{15}N, ^{13}C-labeled proteins, *J. Biomol. NMR* **8,** 351–356 (1996).
12. S. Uhrínová, D. Uhrín, H. Denton, M. Smith, L. Sawyer, and P. N. Barlow, Complete assignment of ^{1}H, ^{13}C and ^{15}N chemical shifts for bovine β-lactoglobulin: Secondary structure and topology of the native state is retained in a partially unfolded form, *J. Biomol. NMR* **12,** 89–107 (1998).
13. S. Uhrínová, D. Uhrín, J. Nairn, N. C. Price, L. A. Fothergill-Gilmore, and P. N. Barlow, Backbone assignment of double labelled 23.7 kDa phosphoglycerate mutase from *Schizosaccharomyces pombe, J. Biomol. NMR* **10,** 309–310 (1997).
14. J. Santoro and G. C. King, A constant-time 2D overbodenhausen experiment for inverse correlation of isotopically enriched species, *J. Magn. Reson.* **97,** 202–207 (1992).
15. G. W. Vuister and A. Bax, Resolution enhancement and spectral editing of uniformly ^{13}C-enriched proteins by homonuclear broadband ^{13}C decoupling, *J. Magn. Reson.* **98,** 428–435 (1992).
16. L. K. Nicholson, L. E. Kay, D. M. Baldisseri, J. Arango, P. E. Young, A. Bax, and D. A. Torchia, Dynamics of methyl-groups in proteins as studied by proton-detected ^{13}C-NMR-spectroscopy. Application to the leucine residues of Staphylococcal nuclease, *Biochemistry* **31,** 5253–5263 (1992).
17. A. Bax, M. Ikura, L. E. Kay, D. A. Torchia, and R. Tschudin, Comparison of different modes of two-dimensional reverse-correlation NMR for the study of proteins. *J. Magn. Reson.* **86,** 304–318 (1990).
18. T. Domke and D. Leibfritz, Reverse editing of protons according to multiplicity (REPAY), *J. Magn. Reson.* **88,** 401–405 (1990).
19. P. Smieder, M. Leidert, M. Kelly, and H. Oschkinat, Multiplicity-selective coherence transfer steps for the design of amino acid-selective experiments—A triple-resonance experiment selective for Asn and Gln, *J. Magn. Reson.* **131,** 199–202 (1998).
20. H. Kessler, P. Schmieder, M. Kock, and M. Regeliu, Selection of methyl resonances in proton-detected heteronuclear shift correlation, the HQQC experiment. *J. Magn. Reson.* **91,** 375–379 (1991).
21. A. Mohebbi, and A. J. Shaka, Improvements in ^{13}C broad-band homonuclear cross-polarization for 2D and 3D NMR, *Chem. Phys. Lett.* **178,** 374–377 (1991).
22. M. Piotto, V. Saudek, and V. Sklenar, Gradient-tailored excitation for single-quantum NMR-spectroscopy of aqueous solutions, *J. Biomol. NMR* **2,** 661–665 (1992).
23. J. Boyd and N. Soffe, Selective excitation by pulse shaping combined with phase modulation, *J. Magn. Reson.* **85,** 406–413 (1989).
24. A. J. Shaka, J. Keeler, T. Frenkiel, and R. Freeman, An improved sequence for broadband decoupling—WALTZ-16, *J. Magn. Reson.* **52,** 335–338 (1983).
25. M. A. McCoy and L. Mueller, Selective shaped pulse decoupling in NMR—homonuclear [C-13] carbonyl decoupling, *J. Am. Chem. Soc.* **114,** 2108–2112 (1992).
26. D. J. States, R. A. Haberkorn, and D. J. Ruben, A two-dimensional nuclear Overhauser experiment with pure absorption phase in four quadrants, *J. Magn. Reson.* **48,** 286–292 (1982).
27. D. Marion, M. Ikura, R. Tschudin, and A. Bax, Rapid recording of 2D NMR spectra without phase cycling—Application to the study of hydrogen exchange in proteins, *J. Magn. Reson.* **85,** 393–399 (1989).